Kidney International, Vol. 60 (2001), pp. 680–693

"Avian-type" renal medullary tubule organization causes immaturity of urine-concentrating ability in neonates

Wen Liu,[1] Tetsuji Morimoto,[1] Yoshiaki Kondo, Kazuie Iinuma, Shinichi Uchida, and Masashi Imai

Department of Pediatrics, Tohoku University School of Medicine, Sendai, Miyagi; Second Department of Internal Medicine, Tokyo Medical and Dental University, Tokyo; and Department of Pharmacology, Jichi Medical College, Kawachi, Tochigi, Japan

"Avian-type" renal medullary tubule organization causes immaturity of urine-concentrating ability in neonates.

Background. While neonatal kidneys are not powerful in concentrating urine, they already dilute urine as efficiently as adult kidneys. To elucidate the basis for this paradoxical immaturity in urine-concentrating ability, we investigated the function of Henle's loop and collecting ducts (IMCDs) in the inner medulla of neonatal rat kidneys.

Methods. Analyses of individual renal tubules in the inner medulla of neonatal and adult rat kidneys were performed by measuring mRNA expression of membrane transporters, transepithelial voltages, and isotopic water and ion fluxes. Immunofluorescent identification of the rCCC2 and rCLC-K1 using polyclonal antibodies was also performed in neonatal and adult kidney slices.

Results. On day 1, the transepithelial voltages (V_{Ts}) in the thin ascending limbs (tALs) and IMCDs were 14.6 ± 1.1 mV ($N = 27$) and −42.7 ± 6.1 mV ($N = 14$), respectively. The V_{Ts} in the thin descending limbs (tDLs) were zero on day 1. The V_{Ts} in the tALs were strongly inhibited by luminal bumetanide or basolateral ouabain, suggesting the presence of a NaCl reabsorption mechanism similar to that in the thick ascending limb (TAL). The diffusional voltage (V_D) of the tAL due to transepithelial NaCl gradient was almost insensitive to a chloride channel blocker 5-nitro-2-(3-phenylpropylamino)-benzoate (NPPB). The V_{Ts} in the IMCDs were strongly inhibited by luminal amiloride.

On day 1, both the tDL and tAL were impermeable to water, indicating the water impermeability of the entire loop. Diffusional water permeability (P_{dw}) and urea permeabilities (P_{urea}) in the IMCDs indicated virtual impermeability to water and urea on day 1. Stimulation by vasopressin (1 nmol/L) revealed that only P_{dw} was sensitive to vasopressin by day 14. A partial isoosmolar replacement of luminal urea by NaCl evoked negligible water flux across the neonatal IMCDs, indicating the absence of urea-dependent volume flux in the neonatal IMCD. These transport characteristics in each neonatal tubule are similar to those in quail kidneys. Identification of mRNAs and immunofluorescent studies for specific transporters, including rAQP-1, rCCC2, rCLC-K1, rENaC β subunit, rAQP-2, and rUT-A1, supported these findings.

Conclusion. We hypothesize that the renal medullary tubule organization of neonatal rats shares a tremendous similarity with avian renal medulla. The qualitative changes in the organization of medullary tubules may be primarily responsible for the immature urine-concentrating ability in mammalian neonates.

Is the "avian-type" renal medulla a component of mammalian newborn kidneys? Our present data on the renal tubular function in neonatal rats have led to a very striking and intriguing hypothesis. Mammalian neonates already possess an almost mature urine-diluting ability at birth [1]. However, the neonates of human and rats can produce hypertonic urine at concentrations only as high as 400 and 600 mOsm/kg, respectively [1]. These observations indicate that the urine-concentrating ability is very immature at birth [2]. Therefore, a paradox exists that the kidneys have a poor concentrating ability in spite of a mature urine-diluting ability at birth. Many reports have attempted to explain the immaturity of the urine-concentrating ability of neonates [1]. These reports have attributed the immaturity to a short Henle's loop, decreased medullary tonicity, increased production of prostaglandins, and a reduced vasopressin-elicited water permeability response of the collecting duct [1]. None of them, however, have fully accounted for the paradox noted above.

It was first reported in the 19th century that morphologically, neonatal kidneys do not possess inner medullae [3]. However, the details of this observation were not well documented at that time due to the limitations in the application of the experimental technologies.

In addition, the finding that Henle's loop in the super-

[1] These authors contributed equally to this study.

Key words: kidney medulla, fetal kidney, ontogeny, phylogeny, Henle's loop, collecting duct, growth and development.

Received for publication June 8, 2000
and in revised form February 23, 2001
Accepted for publication March 6, 2001

ficial nephron of rat kidneys does not penetrate the outer medulla at birth supports a further hypothesis that the absence of the loop in the superficial nephron at birth is the cause of immaturity in the urine concentration mechanism [2]. However, this latter hypothesis does not provide a conclusion as to why the immature organization of the loop in the outer medulla fails to establish the osmotic gradient in the inner medulla.

Recently, Kim et al shed light on the subject by reporting that the thin ascending limb (tAL) of Henle's loop in neonatal rats is also morphologically different from that in adults [4]. Their group revealed that the tAL in the neonatal period is quite similar to the thick ascending limb (TAL) and that the tubule is replaced by the mature tAL cells after apoptosis and transformation [4].

The tAL, the first diluting segment of Henle's loop, dilutes urine flowing out into the renal medulla with passive NaCl extrusion [5] via a paracellular Na^+ shunt [6] and rCLC-K1 Cl^- channel [7]. Our collaborative studies revealed that the knockout of the Cl^- channel rCLC-K1 gene leads to severe nephrogenic diabetes insipidus in mice [8]. Taken together, these studies clearly show that the presence of the tAL is essential for normal urine-concentrating ability in mammals. From this knowledge, we can presume that the lack of normal function of the tAL in the neonatal renal medulla also leads to a poor urine-concentrating ability.

Recent molecular biological studies revealed that the subunits of the epithelial sodium channel (ENaC), an amiloride-sensitive Na^+ channel, are expressed in the IMCD in the fetal and early neonatal periods [9]. It is also known that aquaporin-1 (AQP-1), the high-capacity water channel, is not expressed in the fetal descending thin limb (tDL) [10]. These molecular biological findings imply that the urine-concentrating mechanism in the neonatal period may be different from that in mature kidneys.

Direct examination of the function of the renal tubule is crucial for the elucidation of the precise mechanism thus far; the investigation of separate transporters such as water channels, ion transporters, and urea transporters has not adequately demonstrated the presence of unknown transport systems that might compensate for the alteration of the expression of known transport systems. To elucidate the precise mechanism, we examined the function of the renal tubule directly in a series of experiments using in vitro tubule microperfusion and reverse transcription-polymerase chain reaction (RT-PCR) detection of mRNAs for known transporters in the isolated inner medullary tubules of fetal, neonatal, and adult rat kidneys.

The results of our studies have led us to a striking new concept about the maturing mechanism in the urine-concentrating ability of mammalian neonates.

METHODS

Immunohistological analyses

Single nephron segments were microdissected with fine forceps in ice-cold dissection solution containing (in mmol/L) 135 NaCl, 5 KCl, 0.1 Na_2HPO_4, 0.12 Na_2SO_4, 2.5 $CaCl_2$, 1.2 $MgSO_4$, 5 N-2-hydroxyethylpiperazine-N′-2-ethanesulfonic acid (HEPES), 5.5 glucose, 0.3 sodium acetate, and 10 vanadyl ribonucleoside complex (VRC; Life Technologies, Grand Island, NY, USA), a potent RNase inhibitor. VRC was centrifuged prior to use to remove the solid phase. The pH of solution was adjusted to 7.4 with NaOH. After dissection, nephron segments were rinsed in the same solution without VRC and transferred in 2 μL aliquots to tubes containing 6.7 μL of 2% Triton X-100 (Sigma Chemical, St. Louis, MO, USA) to permeabilize the cells, 1.2 U/μL placental RNase inhibitor (Takara), and 5 mmol/L dithiothreitol (Boehringer Mannheim, Mannheim, Germany). A total tubule length of 0.8 to 1.0 mm was placed in each tubule preparation. The tubules were frozen at −80°C until their use within two hours at room temperature.

Rat kidneys were perfused with 2% paraformaldehyde and immersed overnight. Fifty micrometer sections were cut with a MICROSLICER DTK-1000 (Douhan, E.M., Kyoto, Japan) and thaw mounted on silane-coated glass slides (Muto Pure Chemicals Co., Ltd., Tokyo, Japan). Immunostaining was performed using a TSA-direct kit (NEN Life Science Products, Boston, MA, USA) according to the manufacturer's instructions. Sections were examined with a FLUOVIEW laser-scanning microscope (Olympus, Tokyo, Japan). Anti-rat rCLC-K1 antibody (1:200) and anti-rat rCCC2 antibody (1:500) were used for the detection of rat rCLC-K1 and rCCC2 as the first antibodies. The polyclonal antibody for rCCC2 was a generous gift from Dr. Steven C. Hebert.

RT-PCR reactions

A slightly modified version of the method of Moriyama et al was used for qualitative localization of rAQP-1, rCLC-K1, rCCC2, rENaC β subunit, rAQP-2, rUT-A1, and β-actin mRNAs [11]. The specific primers used for rAQP1 were antisense, 5′-CTA TTT GGG CTT CAT CTC CAC CC-3′ corresponding to bases 810 to 788 from ATG, and sense 5′-CAT GAC CCT CTT CGT CTT CAT CAG-3′ corresponding to bases 60 to 83 from ATG on the reported cDNA sequence [12]. The specific primers used for rCLC-K1 were antisense, 5′-CTG TTC TGA CCC CAA CGC TG-3′ corresponding to bases 2086 to 2067 from ATG, and sense, 5′-TCT CCA GGA CAT CTT GGC AGG-3′ corresponding to bases 1851 to 1871 from ATG on the cDNA sequence reported by Uchida et al [13]. The specific primers used for rCCC2 were antisense, 5′-CAA CAT TTC TCA TCC CTC GCG C-3′ corresponding to bases 3311 to 3289 from ATG, and

sense, 5′-CTC CAC GAA AGC CAC AAA GAT-3′ corresponding to bases 2986 to 3006 from ATG on the reported cDNA sequence [14]. The specific primers used for the rENaC β subunit were antisense, 5′-ACT CAA TGA GGC ACA GCA CCG-3′ corresponding to bases 1612 to 1592 from ATG, and sense, 5′-CTG GGG AGA AAT ACT GCA AC-3′ corresponding to bases 1223 to 1242 from ATG on the reported cDNA sequence [9]. The specific primers used for AQP2 were antisense, 5′-TAA GCA CAG TCC CCC AGA AGG-3′ corresponding to bases 1111 to 1131 from ATG, and sense 5′-TCC AGC AGT TGT CAC TGG C-3′ corresponding to bases 570 to 588 from ATG on the cDNA sequence reported by Fushimi et al [15]. The specific primers used for rUT-A1 were antisense, 5′-TCC GTG TGA CTG TTC TCC-3′ corresponding to bases 1777 to 1760 from ATG, and sense 5′-GTT TCC TGT GAC CTT CGC ATC C-3′ corresponding to bases 1021 to 1042 from ATG on the cDNA sequence [16]. The sense primer for rat β-actin was 5′-TAC AAC CTC CTT GCA GCT CC-3′ in the 5′ untranslated region of exon 1 of the rat β-actin gene. The reverse primer 5′-GGA TCT TCA TGA GGT AGT CTG TC-3′ corresponds to a 23-nucleotide sequence from exon 4 of the rat β-actin gene. Based on published sequences, these primers are predicted to amplify 630 bp fragments of rat β-actin reverse-transcribed mRNA [17]. The anticipated PCR products of rAQP-1, rCLC-K1, rCCC2, rENaC β subunits, rAQP-2, rUT-A1, and β-actin have a length of 751, 236, 326, 391, 562, 757, and 630 bp, respectively. RT-PCR was carried out using a Thermoscript™ RT-PCR Kit (GIBCO BRL, Grand Island, NY, USA) according to the manufacturer's protocol. For RT-PCR, the tubule segments frozen in permeabilizing solution were thawed, and 10 μL of a master mix containing 5 U of RNase inhibitor, 0.2 mmol/L of each deoxynucleotide triphosphate (dNTP), 5 mmol/L dithiothreitol, 0.5 pmol of oligo-dT primer, and sterile water were added to each tube. Next, the tubes were incubated at 50°C for 30 minutes to carry out the reverse transcription. The PCR reactions were performed using the GeneAmp PCR System 2400 (Perkin-Elmer, Foster City, CA, USA). After an initial melt for two minutes at 94°C, the PCR process underwent 30 cycles of 30 seconds at 94°C, 30 seconds at 60°C, and 45 seconds at 68°C, followed by a final extension for seven minutes at 68°C. The PCR products were size fractionated by electrophoresis on 1.5% agarose gel and visualized by ethidium bromide staining.

Isolation and microperfusion of renal tubules

Pregnant, newborn, and adult rats were anesthetized with intraperitoneal pentobarbital, and their left kidneys were removed. The renal tubule segment was microdissected with fine forceps under a stereoscopic microscope. The border between the outer and inner medulla in neonatal and adult kidneys was identified macroscopically as previously reported by Kim et al [4]. To avoid contamination of the tubules originating from the outer medulla, the inner two thirds of the inner medulla in both neonatal and adult kidneys were used for microdissection of the tubule fragments. A fragment of the tubule was transferred to a chamber on the stage of an inverted microscope and was microperfused in vitro at 37°C using Burg et al's method [18] with some modifications. Both sides of the tubule were initially microperfused with HEPES-buffered Ringer solution containing (in mmol/L) 135 NaCl, 3.0 KCl, 2.0 KH_2PO_4, 1.5 $CaCl_2$, 1.0 $MgCl_2$, 10 HEPES, 100 urea, 1.0 sodium acetate, 5.5 glucose, and 5.0 L alanine. The solution was titrated to pH 7.4 with NaOH at 37°C. In the experiments with bicarbonate-buffered solutions, both sides of the tubules were microperfused with bicarbonated-buffered Ringer's solution containing (in mmol/L) 110 NaCl, 5.0 KCl, 1.2 Na_2HPO_4, 0.8 NaH_2PO_4, 1.5 $CaCl_2$, 1.0 $MgCl_2$, 25 $NaHCO_3$, 100 urea, 1.0 sodium acetate, 5.5 glucose, and 5.0 L alanine. The bicarbonate-buffered solution was bubbled with 5% CO_2 to keep the pH 7.4 at 37°C. The perfusion rate of the luminal solution in the studies for spontaneous transepithelial voltage measurements was kept as low as 5 nL/min. In the experiments measuring the transepithelial diffusional voltages of Na^+ and Cl^-, the perfusion rate was kept above 20 nL/min to avoid the dissipation of transepithelial gradients of solution composition across the tubules.

Measurement of transepithelial potentials

The transepithelial voltage (V_T) was measured by connecting the bath and perfusion pipette via a saturated KCl flowing boundary and NaCl Ringer-containing agar bridge, respectively. A high-input impedance electrometer was used to monitor the V_{Ts} (Duo773; WP Instruments, New Haven, CT, USA). To measure diffusional potential (V_D) evoked by the transepithelial electrolyte gradient, the bath solution was exchanged with another HEPES-buffered Ringer's solution containing (in mmol/L) 65 NaCl, 3.0 KCl, 2.0 KH_2PO_4, 1.5 $CaCl_2$, 1.0 $MgCl_2$, 10 HEPES, 230 urea, 1.0 sodium acetate, 5.5 glucose, and 5.0 L alanine, being titrated to pH 7.4 with NaOH at 37°C. The deflections of the V_{Ts} were observed as V_{Ds}. The KCl flowing boundary minimized the changes in liquid junction potential due to solution exchange [19].

Measurement of hydraulic conductivities

For determination of osmotic water permeability (Lp), the tDL was bathed in a hyperosmotic medium containing 50 mmol/L sucrose to induce a transtubular osmotic gradient. After 10 to 15 minutes of equilibration, three to four samples were collected. Lp ($10^{-9} \cdot cm^2 \cdot s^{-1} \cdot atm^{-1}$) was estimated from net water movement

produced by the osmotic gradient according to the following equation:

$$\text{Lp } (10^{-9}\ \text{cm}^2 \cdot \text{s}^{-1} \cdot \text{atm}^{-1}) = \frac{1}{\pi_b L} \cdot \left[(\text{Vi} - \text{Vo}) + \frac{\pi_i \text{Vi}}{\pi_b} \ln \frac{\text{Co}(\pi_b - \pi_i)}{(\text{Ci}\pi_b - \text{Co}\pi_i)} \right]$$

whereVi is the perfusion rate, Vo the collection rate, L the length of the tubule, and Ci and Co the radioactivities (concentration) of ^{3}H in the perfusate and collected fluid, and π_i and π_b are the osmolality (in atm) of the perfusate and the bathing medium, respectively.

Measurement of volume flux

Net water flux (Jv) of the IMCD was measured in a perfusion bath using [Methoxy-^{3}H] inulin as a volume marker (740 mBq/mL perfusate). After equilibration, three to four collections of the perfusate were taken. Jv was calculated as follows:

$$\text{Jv } (\text{nL} \cdot \text{mm}^{-1} \cdot \text{min}^{-1}) = \frac{\text{Vo}}{\text{L}} \left[\frac{\text{Co}}{\text{Ci}} - 1 \right]$$

Measurement of isotopic efflux coefficients or diffusional water permeabilities

Urea and water fluxes from the tubular lumen to the bath were measured as indexes of the tDL and the tAL for diffusional permeabilities to urea and water, whereas compositions of perfusate and bathing fluid were identical. [^{14}C] urea (370 mBq/mL) or [^{3}H] H_2O (740 mBq/mL) was added to the perfusate (final concentration). Both fluxes were determined simultaneously in the same tubule preparations, if the protocol allowed, and the overlap of ^{3}H and ^{14}C radioactivities was corrected when this was done. The lumen-to-bath flux coefficient for the isotope "x" (P_x) was calculated as:

$$P_x\ (\times 10^{-7}\ \text{cm}^2 \cdot \text{s}^{-1}) = \frac{\text{Vo}}{\text{L}} \ln \frac{\text{Ci}^*}{\text{Co}^*}$$

where Ci* and Co* are radioactivities (concentrations) of isotopes in the perfusate and collected fluid, respectively, and the other variables are as shown previously in this article.

Statistical analyses

Data were expressed as mean ± SE. Analysis of variance in combination with the Scheffe's *F* test was performed for comparison of developmental time effects. Otherwise, statistical analyses were performed with the Student paired or unpaired *t* test.

RESULTS

Changes in electrolyte transport characteristics

First, the electrical properties of each nephron segment in the inner medulla were observed.

Transepithelial voltages were observed in the tDLs, tALs, and IMCDs when the tubules were microperfused in vitro in the control HEPES-buffered solution. The results in the tALs and IMCDs are depicted in Figure 1. V_{Ts} in the tDLs were not different from zero at any age (data not shown). In the tALs, the V_{Ts} were 15.2 ± 1.9 mV (N = 6) on fetal day 20, 13.8 ± 1.4 mV (N = 18) on day 0, and 14.6 ± 1.1 mV (N = 27) on day 1. After day 1, the V_{Ts} gradually decreased until almost reaching zero on day 5. As previously reported [20], the V_{Ts} in adult tALs were zero. In the IMCDs, the V_{Ts} were −32.4 ± 5.6 mV (N = 13) on fetal day 20, down to −42.7 ± 6.1 mV (N = 14) on day 1, and progressively higher thereafter until reaching zero. The spontaneous V_{Ts} had almost disappeared by day 14.

Transepithelial voltages in the bicarbonate-buffered solution were also measured in the tALs and IMCDs on day 1. The V_{Ts} in the tALs and IMCDs were 19.9 ± 0.2 (N = 4) and −32.7 ± 6.5 mV (N = 4), respectively. The bicarbonate-buffered condition did not affect the V_{Ts} in the tALs and IMCDs qualitatively.

Transepithelial diffusional potential in the tDLs, tALs, and IMCDs was also measured when either basolateral Na^+ (V_{Ds} for Na^+) or Cl^- (V_{Ds} for Cl^-) concentration was decreased tenfold (Fig. 2). The V_{Ds} for Na^+ in the tDLs, tALs, and IMCDs on day 1 were −8.9 ± 0.7 (N = 17), −13.3 ± 1.1 (N = 13), and −4.8 ± 0.5 (N = 8) mV, respectively. The V_{Ds} for Na^+ tended to increase in both the tDLs and tALs. The V_{Ds} for Cl^- in the tDLs, tALs, and IMCDs on day 1 were 10.9 ± 0.4 (N = 8), 8.6 ± 1.3 (N = 12), and 12.5 ± 0.9 (N = 8) mV, respectively.

To characterize the passive electrical properties of the tAL, we tested the sensitivities of V_T and V_D to various transport inhibitors. The effects of 5-nitro-2-(3-phenylpropylamino)-benzoate (NPPB), the Cl^- channel blocker, on the V_{Ds} were evoked by reducing the basolateral NaCl concentration to a half value in the tAL at various ages (Fig. 3). It has been demonstrated that NPPB is a transport inhibitor for Cl^- channel in the hamster tAL [21]. NPPB is known as a Cl^- channel inhibitor of the basolateral membrane of the thick ascending limb from rabbit and mouse kidneys [22]. The NPPB-sensitive component of VD was zero on days 0 and 1 and gradually increased until nearly reaching adult values on day 14. The data indicate that Cl^- permeability via the rCLC-K1 Cl^- channel is absent in the tAL at birth and thereafter emerges rapidly in the neonatal period.

To characterize the active electrical properties of the tAL, the effects of bumetanide and ouabain on V_{Ts} in the tAL also were examined on day 1 (Fig. 4). Bumetanide is an inhibitor of Na-K-2Cl cotransporter in the TAL [23], and ouabain is a specific inhibitor of ubiquitous Na^+ pump in mammalian cell membranes [24]. Bumetanide at 0.1 mmol/L applied to the lumen significantly inhibited the V_{Ts} of four tALs from 8.1 ± 0.7 to 3.8 ± 0.2, with a

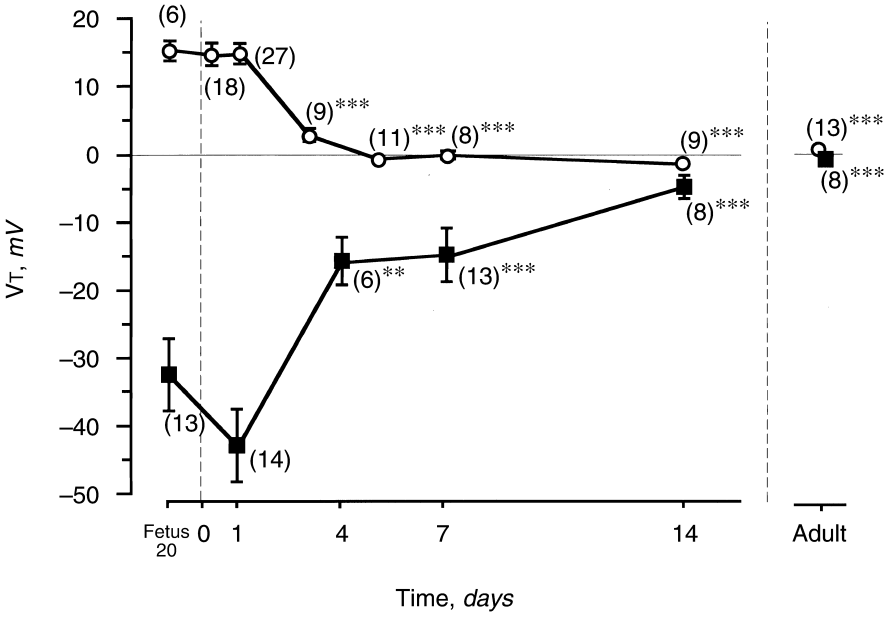

Fig. 1. Changes in the spontaneous voltages of thin ascending limbs (tALs; ○) and inner medullary collecting ducts (IMCDs; ■) in the perinatal period. Changes in spontaneously evoked VTs of the tALs and IMCDs were observed in rats of various ages. The number in parentheses represents number of tubules examined for each point. The transepithelial voltages (V_{Ts}) one day before birth (fetal day 20) in the tALs were 15.2 ± 2.0 (N = 6) mV. On the day of birth, the V_{Ts} in the tALs remained almost constant. The V_{Ts} moved toward zero as the age increased. The V_{Ts} in the tALs almost disappeared on day 5. The V_{Ts} of the IMCDs on fetal day 20 were −32.4 ± 5.6 (N = 13) mV. By the day of birth, the V_{Ts} in the IMCDs were decreased further to −42.7 ± 6.1 mV (N = 14). The V_{Ts} moved toward zero as the age increased. The V_{Ts} in the IMCDs almost disappeared on day 14. $^{**}P < 0.01$; $^{***}P < 0.0001$ vs. day 1.

recovery to 6.6 ± 0.4 mV after washout (Fig. 4A). Ouabain at 1.0 mmol/L inhibited the V_{Ts} of four tALs in the basolateral side from 8.7 ± 1.2 to 4.7 ± 1.3, with a recovery to 6.6 ± 1.0 mV after washout (Fig. 4B). In the bicarbonate-buffered solution, ouabain at 1.0 mmol/L also inhibited V_{Ts} of four tALs in the basolateral side from 21.6 ± 1.9 (N = 4) to 9.2 ± 2.1 (N = 4), with recovery to 20.8 ± 1.5 mV (N = 3) after washout. Application of ouabain and its washout both caused statistically significant changes in VTs ($P < 0.0001$ ouabain vs. control and $P < 0.05$ recovery vs. ouabain). These results indicate the presence of an active NaCl reabsorption mechanism in the tAL at birth.

We also examined the effect of the Na^+ channel blocker amiloride on the V_{Ts} in five IMCDs on day 1 (Fig. 4C). Amiloride at 0.1 mmol/L applied to the lumen of the IMCD diminished the V_{Ts} from −54.4 ± 9.3 to −1.8 ± 0.1, with a recovery to −45.8 ± 8.1 mV after washout. These results indicate that the neonatal IMCDs possess the ability to reabsorb Na^+ actively via electrogenic pathways different from those of adult kidneys. The effect of ouabain on the V_{Ts} in the IMCDs on day 1 was further examined in the bicarbonate-buffered solution. Ouabain at 1.0 mmol/L also inhibited the V_{Ts} of four IMCDs in the basolateral side from −32.7 ± 6.5 (N = 4) to −13.3 ± 5.0 (N = 4), with a recovery to −26.7 ± 7.3 mV (N = 3) after washout. Application and washout of ouabain both caused statistically significant changes in V_{Ts} ($P < 0.002$ ouabain vs. control, $P < 0.05$ recovery vs. ouabain). These data indicate that lumen-negative V_T is due to the presence of an amiloride-sensitive and ouabain-sensitive active transcellular transport process in the neonatal IMCDs.

Changes in water transport characteristics

The examination of specific transporters does not lead to any conclusion on whether water transport itself is present in each nephron segment at each age. To clarify the water transport characteristics in the perinatal period consistently, we measured the diffusional [^{3}H] water permeability (P_{dw}) or hydraulic water conductivity (Lp) in microperfused nephron segments isolated in vitro (Fig. 5).

In the tDL, Lp was measured because P_{dw} was not adequate for comparison due to its extraordinarily high value in mature kidneys (Fig. 5A). Lp was null on day 1, but by day 4 it showed a gradual increase to approximately one-fourth of the value in the adult tDL. By day 14, Lp was already close to the adult value.

In the tAL, P_{dw} values in neonatal and adult rat kidneys were almost the same, suggesting that the tAL is constantly impermeable to water (Fig. 5A).

In the IMCD, the actual water permeability expected from P_{dw} was almost null in the absence of vasopressin on day 1. Stimulation of P_{dw} by vasopressin (1 nmol/L) was already significant on day 1, with a rise in the level from 64.6 ± 12.9 to 93.3 ± 15.3 × 10^{-5} cm · s^{-1} (N = 4, $P < 0.01$). The magnitude of vasopressin's effect on P_{dw} increased with age, and by day 14, the level had nearly reached the same as that in adult, while the IMCD was still impermeable to water in the absence of vasopressin (Fig. 5B).

Changes in urea transport characteristics

To elucidate the characteristics of the urea transport in the inner medullary nephron segments of neonatal rats, the tDLs, tALs, or IMCDs were microperfused in vitro and [^{14}C] urea permeabilities (P_{urea}) were measured (Fig. 6). As shown in Figure 6A, P_{urea} levels in the tAL

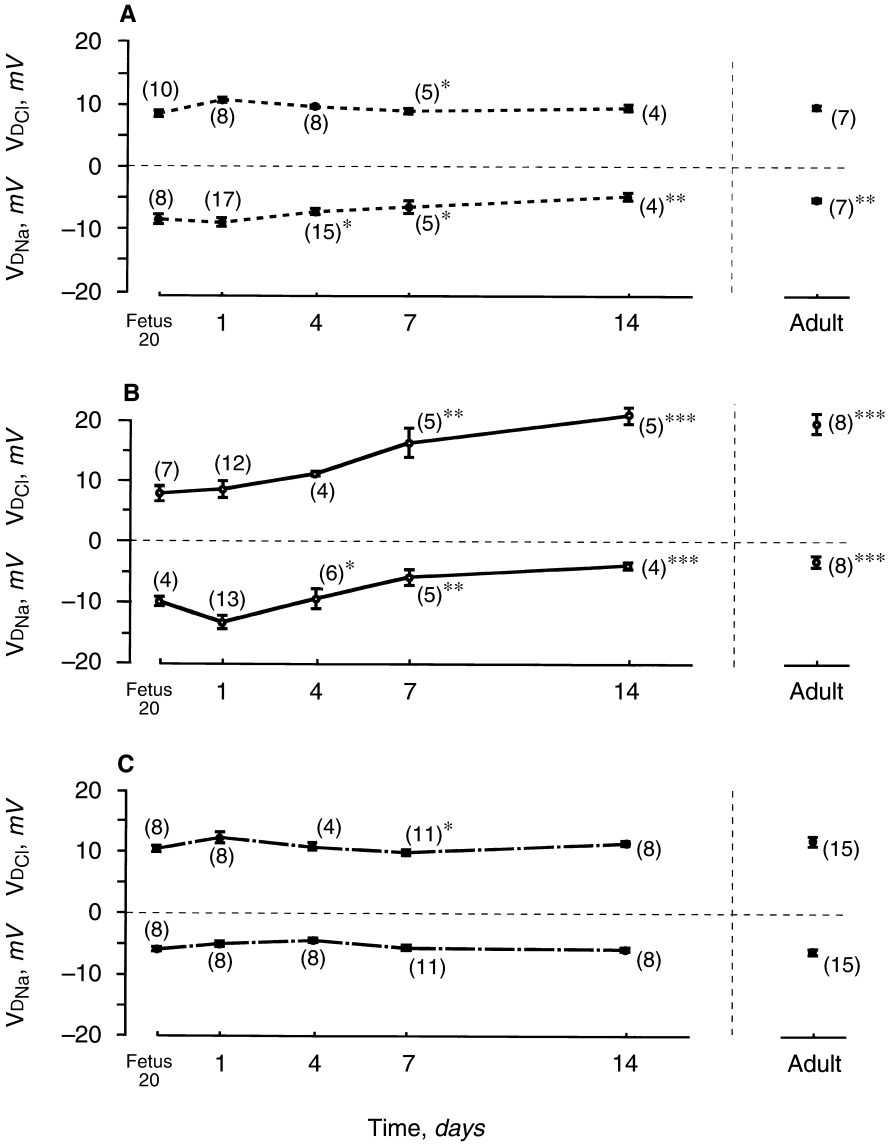

Fig. 2. Changes in transepithelial diffusional voltages. To observe the passive ionic permeabilities of Na^+ and Cl^- in each nephron segment, transepithelial diffusional voltages (V_{Ds}) were measured when basolateral Na^+ or Cl^- concentrations were decreased tenfold by replacement with iso-osmolar N-methyl-D-glucamine and gluconate, respectively. The results in the tDLs, tALs, and IMCDs are depicted in (*A–C*), respectively. The numbers in parentheses represent the numbers of tubules examined for the respective time points. $^*P < 0.05$; $^{**}P < 0.01$; $^{***}P < 0.0001$ vs. day 1.

were much lower than the adult values. P_{urea} in the tAL gradually increased during the neonatal period, while that in the tDL remained almost constant. P_{urea} levels in the tALs were less than half of the adult values at birth and gradually increased during the neonatal period.

We also examined the properties of urea transport in the IMCD (Fig. 6B). To elucidate the characteristics of the entire process of urea transport in the IMCD, the tubule segment was microperfused in vitro and the [^{14}C] P_{urea}s were measured. In the IMCD, P_{urea} was negligible at birth and gradually increased during the neonatal period. P_{urea}'s sensitivity to vasopressin first became significant on day 14, but this sensitivity was still very low.

Comparison of the ability to generate osmotic water flux between newborn and adult

To examine whether urea is utilized as one of the engines for generating osmotic gradient, the presence of urea-driven volume flux in the IMCD was tested (Fig. 7). When there is asymmetry in the urea and NaCl concentrations across the IMCD, the difference between the reflection coefficients of urea and NaCl is known to be an essential driving force inducing the accumulation of urea in the renal medulla [25]. The same experimental protocol was handled in both neonatal and adult rat IMCD. The data clearly show that asymmetry in urea and NaCl across the IMCD does not induce any volume flux in the neonatal IMCD, irrespective of the presence of vasopressin. Thus, there is ample evidence that urea is not utilized for urine concentration in the neonatal IMCD.

RT-PCR identification of major transporters

Recent studies indicate that the rAQP-1 water channel in the tDL is absent in prenatal rat kidneys [26]. To examine the precise changes in the expression of rAQP-1 in

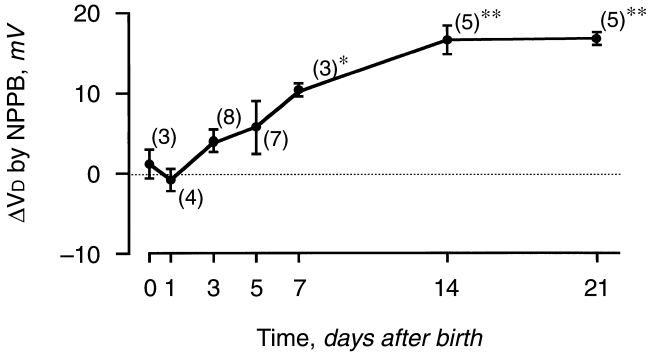

Fig. 3. Changes in NPPB-sensitive components of V_{Ds} in the tALs. To identify the developmental changes in the activity of Cl^- channels in the tALs, NPPB-sensitive components of V_D evoked by transepithelial NaCl gradient were measured in the tALs from rats of various ages microperfused in vitro. To examine the effect of NPPB, 0.1 mmol/L NPPB was added to the bath and the changes in V_{Ds} were observed. The NPPB-sensitive component of V_{Ds} represents the Cl^- channel activity in the tALs. On days 0 and 1, the NPPB-sensitive components of V_{Ds} were null, indicating that Cl^- channels in the tALs are not functionally present in the tALs. The NPPB-sensitive component of the V_{Ds} gradually increased until day 14. The number in parentheses represents the numbers of tubules examined for the respective time points. $^*P < 0.05$; $^{**}P < 0.01$ vs. day 1.

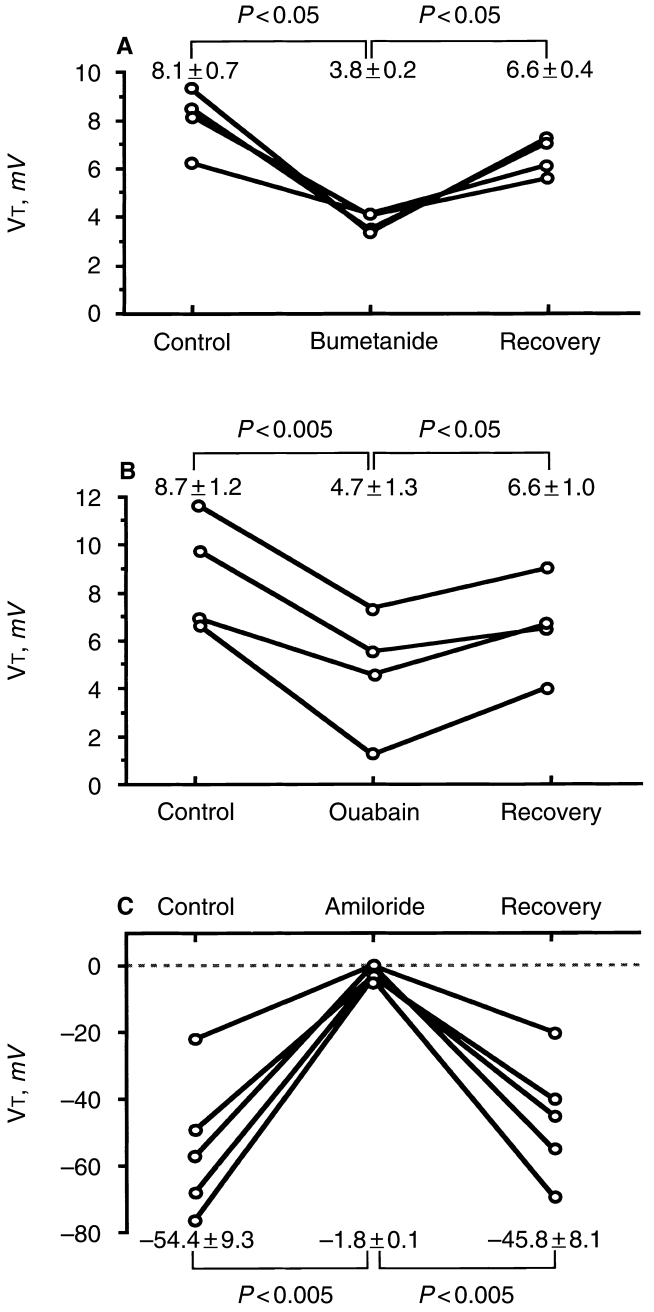

Fig. 4. Sensitivities of transepithelial voltages to inhibitors in the tALs and IMCDs. The effects of (*A*) bumetanide, the inhibitor of the selective Na-K-2Cl cotransporter, and (*B*) ouabain, the specific inhibitor of ubiquitous Na^+ pump, are shown on the tAL of day 1. Doses of 0.1 mmol/L bumetanide in the lumen and 0.1 mmol/L ouabain in the bath significantly inhibited the spontaneously evoked V_{Ts}, indicating that the tAL on day 1 possessed an active Na^+ reabsorption mechanism similar to that of the mature TAL. (*C*) To characterize the properties of negative V_{Ts} of the IMCDs in the early neonatal period, we tested the effect of 0.1 mmol/L amiloride in the lumen on the V_{Ts} in day 1 IMCDs. Amiloride strongly inhibited V_{Ts}, indicating that the active electrogenic Na^+ reabsorption is present in the neonatal IMCDs.

the tDL, the mRNAs for these transporters were identified in isolated tubule fragments by RT-PCR. Rat AQP-1 mRNA in the tDL was merely present at birth and became evident with age (Table 1).

Further tests for the presence of the Cl^- channel rCLC-K1 and the Na-K-2Cl cotransporter rCCC2 were performed by identifying their mRNAs with RT-PCR (Table 1 and Fig. 8). mRNAs for both rCCC2 and rCLC-K1 were present in the tAL on day 1. In the adult rat tAL, mRNA for rCLC-K1 was present, whereas there was only a trace of mRNA for rCCC2.

The vasopressin-sensitive water channel rAQP-2 and urea transporter rUT-A1 has been well established to play significant roles in the reabsorption of water and urea. It also has been reported that fetal and early neonatal IMCDs express each subunit of amiloride-sensitive Na^+ channel rENaC.

To examine the precise changes in the expression of these transporters in the IMCD, the mRNAs for each transporter were identified in isolated tubule fragments by RT-PCR. As in Table 1, the β-subunit of rENaC was present on day 1 and disappeared during the neonatal period. mRNA for rAQP-2 was constantly present in rats of all ages. mRNA for rUT-A1 was virtually undetectable on day 1 and stayed undetectable until late in the neonatal period.

Immunofluorescent identification of rCCC2 and rCLC-K1 in the tAL

Rat CCC2 and rCLC-K1 were identified in immunofluorescent studies using polyclonal antibodies for rCCC2

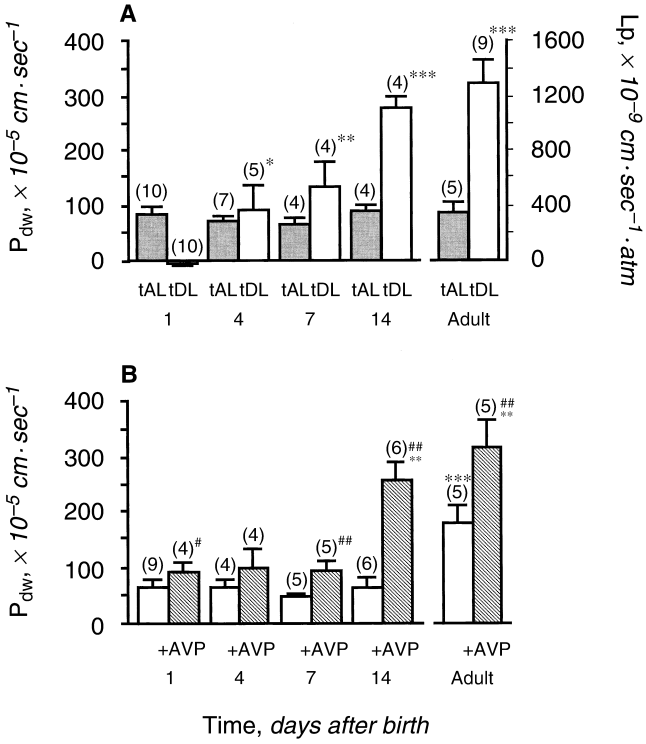

Fig. 5. Changes in water transport. To elucidate the changes in water permeabilites in the tDL, the hydraulic conductivity (Lp) was measured (*A*). The numbers of tubules examined in each period are depicted in parentheses above each column. The Lp in the tDL appeared on day 4 and increased to nearly the adult level by day 14. These results indicate that the tDL is impermeable to water in the early neonatal period. (*B*) To elucidate the changes in water permeabilites in the tAL and IMCDs, the diffusional water permeability (P_{dw}) was also measured. The numbers of tubules examined in each period are depicted above each column. The P_{dw} in the tAL remained constant from day 1 to adulthood, indicating that the tAL is impermeable to water in the neonatal period (A). The changes in basal and vasopressin-stimulated P_{dw} in the IMCDs are depicted in (B). On day 1, the basal P_{dw} was similar to that of the tAL, indicating that the neonatal IMCDs are impermeable to water in the absence of vasopressin. Already on day 1, vasopressin at 1 nmol/L stimulated P_{dw} significantly. While the basal P_{dw} remained low until day 14, the vasopressin-stimulated P_{dw} increased to the adult level by day 14. $^{*}P < 0.05$; $^{**}P < 0.01$; $^{***}P < 0.0001$ vs. day 1; $^{\#}P < 0.05$; $^{\#\#}P < 0.01$ vs. baseline.

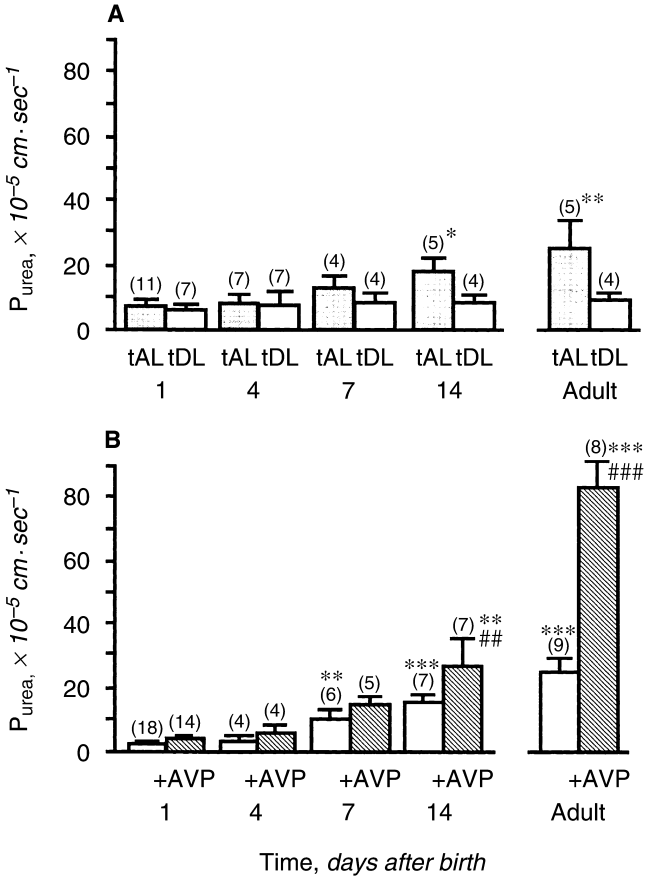

Fig. 6. Changes in urea permeabilities. Changes in the urea permeabilities (P_{urea}) in the tDL and tAL were observed in the tubule preparation microperfused in vitro (*A*). While the P_{urea} in the tDL remained less than 10×10^{-5} cm · s^{-1}, P_{urea} in the tAL gradually increased during the neonatal period, reaching two thirds of the adult value on day 14. Changes in the urea permeabilities (P_{urea}) in the IMCDs were also observed in the tubule preparation microperfused in vitro. (*B*) P_{urea} of the IMCDs in the presence and absence of vasopressin. P_{urea}s in the IMCDs on days 1 and 4 were negligible. The basal P_{urea} appeared on day 7 and was half of the adult value. The stimulation of P_{urea} by vasopressin first became significant on day 14, but the level of stimulation was still less than one third of that in adults. The numbers in parentheses represent the numbers of tubules examined for the respective points. $^{*}P < 0.05$; $^{**}P < 0.01$; $^{***}P < 0.0001$ vs. day 1; $^{\#\#}P < 0.01$; $^{\#\#\#}P < 0.0001$ vs. baseline.

and rCLC-K1 (Fig. 9). While the immunoreactivity of rCCC2 was detected in the entire ascending limb in the newborn rat kidney, it disappeared from the tAL in the adult rat. Immunoreactivity to rCLC-K1 was not detected in newborn rat renal medulla.

DISCUSSION

Maturation of urine-concentrating ability in neonates

Since only a single nephron segment such as the TAL or distal convoluted tubule is capable of extensively lowering the luminal concentration of NaCl, it can be presumed that the dilution of urine requires a less complicated system. This is simply accomplished by the presence of water-impermeable segments with active NaCl reabsorption. On the other hand, urine concentration seems to require a more complicated system because water reabsorption into the body requires a higher osmolarity than the serum. It is therefore crucial for animals to establish hyperosmotic environment in the renal medulla.

Recently, many important transporters of water, electrolytes, and urea in the renal medulla have been identified. These include AQP-1 in the tDL [10], CLC-K1 in the thin ascending limb [7], CCC2 in the TAL [23], and AQP-2 [15], AQP-3, and AQP-4 [10] in the collecting duct. In addition to the established urea transporters

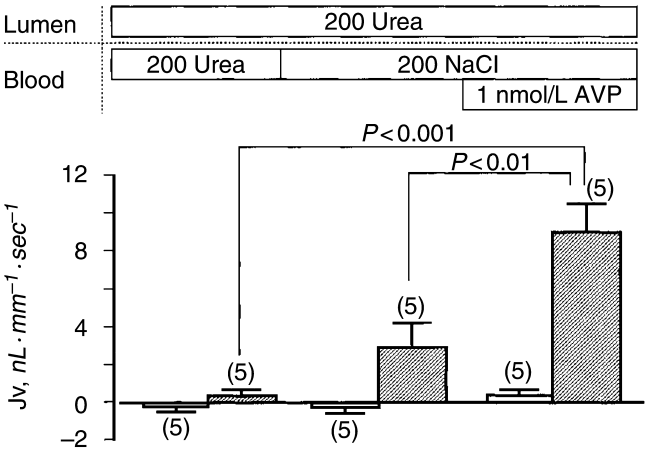

Fig. 7. Urea-dependent volume flux in the neonatal period. Symbols are: (□) day 1; (▨) adult. Isosmotic replacement of luminal NaCl with urea leads to volume efflux (Jv) in the adult IMCDs. It is generally accepted that the Jv induced by such a gradient of NaCl and urea is the most important driving force for the urine-concentrating mechanism via the IMCDs. To elucidate whether the same mechanism plays a role in the neonatal IMCDs, Jv was examined in the presence of transepithelial NaCl and the urea gradient in the neonatal and adult rat IMCDs. Jv in the adult IMCDs was stimulated by both the imposition of transepithelial NaCl and urea gradient, and the sequential stimulation by vasopressin. However, neither maneuver produced a volume flux in the IMCD on day 1. These results clearly indicate that the neonatal IMCDs do not have the ability to reabsorb water by the mechanism using transepithelial reversed NaCl and urea gradient. The number in parentheses represents number of tubules examined for each point.

Table 1. Expression of mRNAs for various transporters in the inner medullary nephron segments

	Age				
	Day 1	Day 4	Day 7	Day 14	Adult
tDL					
rAQP-1	−	+	+	+	+
tAL					
rCLC-K1	+	+	+	+	+
rCCC2	+	+	+	±	±
IMCD					
rNaC β subunit	+	+	+	−	−
rAQP-2	+	+	+	+	+
rUT-A1	−	−	−	+	+

Signs are: +, present; −, absent; ±, trace.

Abbreviations are: tDL, thin descending limb; tAL, thin ascending limb; IMCD, inner medullary collecting duct; AQP, aquaporin; r, rat; CLC-K1, specific chloride channel; NaC, sodium channel; UT, urea transporter.

UT-A1, UT-A2, and UT-A3, researchers have now also identified UT-A4 [27]. While several studies have investigated the expression of these transporters in the neonatal kidneys, none have ever examined their expression in close conjunction with the examination of the overall transport properties of water and electrolytes in each nephron segment. To elucidate how each tubule segment handles water and electrolytes in the neonatal period, the overall function of each tubule must be directly examined. To accomplish this, we examined tubule functions using a direct, in vitro microperfusion technique before identifying the expression of the important transporters for urine concentration by immunofluorescence and RT-PCR.

Several tremendous functional differences of solute and water transport between neonatal and adult rat kidneys were observed. To begin with, several neonatal-specific characteristics were found. This neonatal phase, depicted in Figure 10, has the following characteristics: (*1*) The entire length of the descending limb is impermeable to water on days 0 and 1 of neonatal rats, indicating that the descending limb does not contribute to water movement across this segment. Taken together with the result that the neonatal tAL is also impermeable to water, there must be no reabsorption of water in neonatal Henle's loop. Therefore, the mechanism of water reabsorption in the neonatal inner medulla is qualitatively different from that in mature mammals. (*2*) The tAL possesses an active NaCl reabsorption mechanism quite similar to that in the TAL, and though the mRNA for the tAL-specific Cl^- channel rCLC-K1 is already present at birth, rCLC-K1 itself is functionally absent. Therefore, the tAL reabsorbs NaCl by a completely different mechanism from that in the mature tAL. (*3*) The urea permeability is much lower in the neonatal tAL, suggesting that urea transport in Henle's loop may not contribute to urine concentration in neonatal rats. (*4*) Amiloride-sensitive active Na^+ reabsorption is present in the IMCD. (*5*) Basal and vasopressin-stimulated urea permeability in the IMCD is almost negligible.

Considering these new results, we conclude that there is a specific phase in the maturation of the inner medulla characterized by the simple and active accumulation of NaCl into the renal medulla. This constitutes a large difference from the mature system. First of all, mature Henle's loop reabsorbs not just NaCl across the epithelium, but also water and urea. Second, unlike the mature IMCD, the neonatal IMCD is hindered from recycling urea in the inner medulla.

We postulate, therefore, that there is a qualitatively distinct phase in the organization of the inner medulla early in the neonatal period.

Another intriguing aspect is that the expression of transport properties may be classified into two groups.

The first, a group of transport properties already present at birth that disappear soon thereafter, includes active NaCl reabsorption in the tAL and active Na^+ reabsorption in the IMCD. The former property is represented by the luminal rCCC2 and basolateral Na^+,K^+-ATPase, just as in the mature TAL, and the latter occurs via the amiloride-sensitive Na^+ channel in the luminal membrane of the IMCD.

The second is a group of transport properties that emerge late after birth. These include water permeability of the tDL with rAQP-1, passive Cl^- permeability with

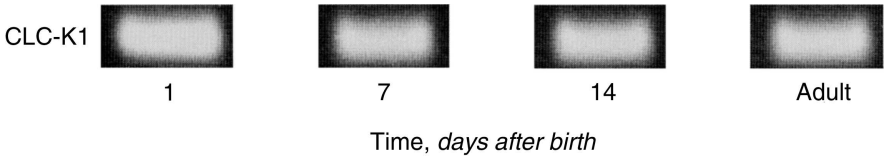

Fig. 8. Changes in mRNA expression of rCLC-K1. RT-PCR was used to measure mRNAs for rCLC-K1 in the tAL. The amount of mRNA for each 1.5 mm length of the nephron segment was identified. The strong expression of mRNA for the rCLC-K1 Cl^- channel was already identified in the tAL on day 1 and constantly present there until adulthood. The results of identification of mRNAs for major transporters in each segment are summarized in Table 1.

rCLC-K1 in the tAL, vasopressin-sensitive urea permeability with rUT-A1, and urea permeabilities of Henle's loop. The features of the second group suggest that the transport properties in the first group are overwritten and replaced. Among the second group, it is noteworthy that the development of vasopressin-sensitive urea permeability in the IMCD is still far from complete on day 14, when almost all other transport properties in the second group accomplish their maturation. The development of vasopressin-sensitive urea permeability may be the late-period limiting factor for the maturation of urine concentration in the entire maternal feeding interval.

Our present study demonstrates that the mRNA for rCLC-K1 is already present in the tAL at birth in spite of the absence of Cl^- permeability via the rCLC-K1 Cl^- channel. In our preliminary immunohistochemical study, the immunoreactivity for rCLC-K1 was absent in the tAL at birth. When considering these results in total, it appears that there may be an interruption in the transcription of rCLC-K1 peptide from mRNA in the tAL cells at birth. Further studies are required to elucidate how such a discrepant phenomenon occurs.

Ontogenetic and phylogenetic aspects of urine concentration

The present data also imply some intriguing aspects in understanding the ontogeny and phylogeny of the urine-concentrating mechanism in mammals.

The classic phylogeny based on the fossil records is constructed around a central thesis that birds and mammals inherited entirely separate traits as they diverged from reptiles [28]. Recent morphological phylogeny, however, challenges the classic fossil-based concept by indicating some common traits between mammals and birds [29], such as a single aortic trunk, folded cerebellum, scroll-like turbinals, Henle's loop in kidneys, adventitious cartilage, and endothermy [29]. Although recent molecular biological approaches demonstrate that birds are more closely related to crocodilians and squamates such as lizards and snakes [30] than to mammals, the traits they share with mammals still raise considerable questions regarding the relationship between these two classes of vertebrates.

The kidneys of mature mammals and birds both derive from metanephros [31]. Nephrons in each class of vertebrates are composed of two types, that is, short-looped and long-looped nephrons in mammals [32], and reptilian-type and mammalian-type nephrons in birds [33]. Henle's loop is present in both nephrons in mammals and in mammalian-type nephron in birds. The major morphological difference of Henle's loop between mammals and birds is the presence of the long-looped nephron possessing the ascending thin limb (tAL) in the former.

From the 1980s, Nishimura et al examined the precise function of renal medullary tubules in avian kidneys [34–37]. Over the course of several years, these authors demonstrated the basic transport characteristics of each medullary nephron segment in quail. The avian thin descending limb is permeable to NaCl and virtually impermeable to water [36], while the mammalian thin limb is extraordinarily permeable to water. The avian ascending limb has a low osmotic water permeability accompanied by net NaCl reabsorption and low passive Cl^- permeability, indicating that the tAL functions as an active diluting segment [35].

However, we know that the loops of mammals and birds are functionally very different since the descending loop in the former is highly permeable to water, while the entire loop in the latter is impermeable to water [36]. The only tAL with a large passive NaCl permeability is present in the mammalian ascending limb of Henle's loop. Arginine vasotocin increases water permeability in the medullary collecting duct (MCD) in a manner similar to vasopressin in mammals [37]. Stanton reported that in the initial portion of the IMCD from adult rats, ouabain significantly depolarized both lumen-negative transepithelial and basolateral membrane voltages, indicating that the initial IMCD of the adult rat kidney also possesses an active reabsorption process of Na^+ via the basolateral Na^+ pump [38]. Imai and Yoshitomi reported that in the middle portion of the IMCD from hamster's kidneys, the apical membrane possesses the amiloride-sensitive Na^+ conductance and the basolateral membrane has the ouabain-sensitive Na^+ pump, although both are too small to play a physiological role in the transepithelial Na^+ transport [39]. While the amount of

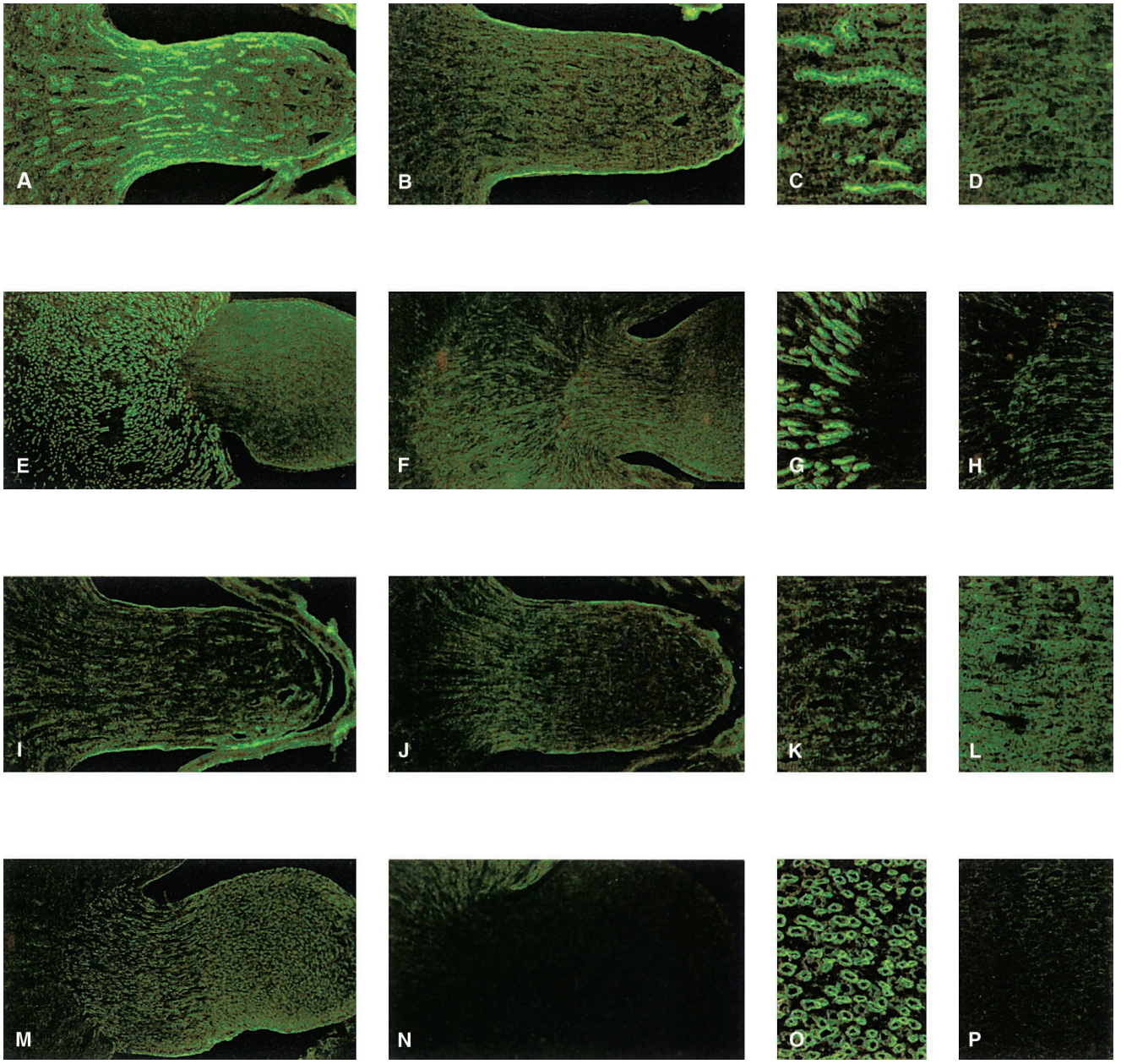

Fig. 9. Immunofluorescent detection of rCCC2 and rCLC-K1 in the loop of Henle. In addition to detection of the mRNA for both rCCC2 and rCLC-K1 in Henle's loop, the distribution of antigenicity of both transporters was detected by using their polyclonal antibodies. The immunofluorescent staining for rCCC2 and its preimmune serum are depicted in *A, C, E,* and *G*, and in *B, D, F,* and *H*, respectively. Those for rCLC-K1 and its control are depicted in *I, K, M,* and *O*, and in *J, L, N,* and *P*, respectively. On day 1, the immunoreactivity for rCCC2 was detected in the entire medulla (A and C), while that for rCLC-K1 was entirely absent (I and K). In contrast, immunoreactivity for rCCC2 in the adult kidneys was present only in the outer medulla (E and G). The immunoreactivity for rCLC-K1 in the adult kidneys was present exclusively in the inner medulla (M and O). These results indicate that rCCC2 is present in the entire medulla at birth, but soon thereafter dissipates from the inner medulla and is replaced by rCLC-K1 in the tAL. The observation for preimmune serum for both rCCC2 and rCLC-K1 are depicted, where both J and K are on day 1, L and M are in the adult kidneys, J and L are for rCCC2, and K and M are for rCLC-K1. (Magnifications: ×100 in A, B, I, and J; ×400 in C, D, G, H, K, L, O, and P; ×40 in E, F, M, and N)

active Na^+ transport is significant only in the initial portion of the mammalian IMCD, electrogenic Na^+ reabsorption is present in the avian MCD [40]. These observations suggest that there is an obvious difference in the transport characteristics of the medullary collecting ducts of mammalian and avian kidneys.

These major differences in the functions of the renal tubule in the medulla have suggested the possibility that the Henle's loops in mammals and birds are two entirely distinct systems that emerged independently in the process of evolution.

However, our astonishing observation is that the neo-

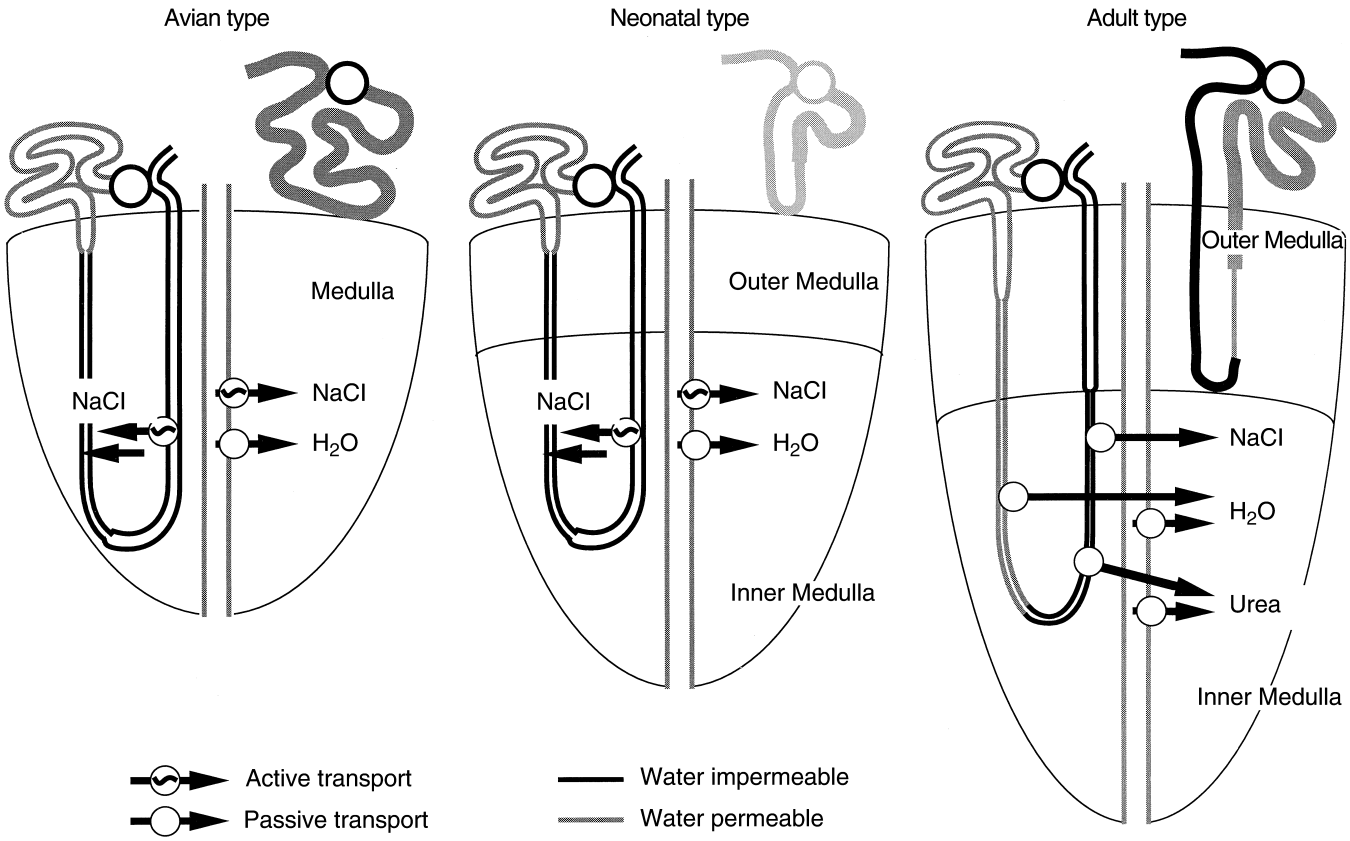

Fig. 10. Proposed concept for the qualitative maturation of the urine-concentrating mechanism in neonatal rat kidneys. It is known that only one type of nephron, the long-looped nephron, possesses the Henle's loop in the neonatal renal medulla. The neonatal Henle's loop is impermeable to water throughout its entire length and only accumulates NaCl actively in the medulla. Although the water permeability of the IMCD is stimulated by vasopressin at birth, the urea permeability is negligible. In view of the tremendous similarities to the avian renal medulla, this 'neonatal-type' of tubule organization can be considered an "avian-type." The maturation of the inner medulla may be divided into two coexistent groups of events involving changes in the properties of renal tubules. One is the disappearance of "neonatal-type" transport properties, that is, the bumetanide-sensitive active NaCl reabsorption in the tAL, and the amiloride-sensitive Na^+ reabsorption in the IMCD. Another is the emergence of three "mammalian-type" transport properties, that is, water permeability in the tDL, passive NaCl permeability in the tAL, and vasopressin-sensitive urea permeability in the IMCD. The maturation of the urine-concentrating system in the inner medulla can be accurately characterized as an overwriting of the "neonatal-type" or "avian-type" transport properties with the "mammalian-type" systems. We therefore postulate a new model for the maturation process of urine-concentrating system in which the "avian-type" renal medullary tubule organization is responsible for the immaturity of the urine-concentrating ability in neonates.

natal medulla temporarily acquires a tubule organization very similar to that in the avian medulla. During the brief period when this organization is acquired, Henle's loop is impermeable to water, the IMCD possesses an amiloride-sensitive Na^+ reabsorption mechanism, and urea transport remains undeveloped in the IMCD. Nishimura et al intensively examined the function of the MCDs in quail kidneys [37, 40]. They revealed vasotocin-sensitive low water permeability and lumen-negative electrogenic Na reabsorption in the quail MCDs. These two characteristics, together with the low urea permeability of the avian MCDs, resemble the characteristics of mammalian neonatal IMCDs. Therefore, these features of tubular transport properties in all the inner medullary nephron segments closely resemble the avian medullary function. If we step back to take a broader view of this issue, it is notable that the superficial nephron of rat kidney does not possess Henle's loop in the medulla at birth and that its loop penetrates the medulla late in the neonatal period. Given this finding, we know that the morphological and functional organization of Henle's loop and IMCD in the neonatal rat corresponds to that in birds. We therefore dare to label the organization of the neonatal medulla the "avian-type," and postulate that the neonatal period is a period of functional conversion of the urine-concentrating mechanism from the "avian type" to the real "mammalian type." Although our data do not provide definite evidence regarding the phylogeny of Henle's loop in mammals and birds, we propose with relative assurance that the "mammalian-

type" urine-concentrating mechanism is established after the "avian-type" phase.

ACKNOWLEDGMENTS

This work was supported in part by a grant-in-aid from the Ministry of Education, Science and Culture of Japan, and by a research grant from the Salt Science Research Foundation in Japan. We thank Drs. M. Nagata and C.N. Inoue for their excellent criticism. We thank Ms. Naoko Sato for her excellent technical assistance. A preliminary account of a portion of this study was communicated to the XXXII Meeting of the American Society of Nephrology (1999).

Reprint requests to Yoshiaki Kondo, M.D., Ph.D., Department of Pediatrics, Tohoku University School of Medicine, Seiryo-machi, Aoba-ku, Sendai, Miyagi 980-8574, Japan.
E-mail: ykondo@ped.med.tohoku.ac.jp

APPENDIX

Abbreviations used in this article are: AQP, aquaporin; dNTP, deoxynucleotide triphosphate; ENaC, epithelial sodium channel; IMCD, inner medullary collecting duct; tAL, thin ascending limb; MCD, medullary collecting duct; NPPB, 5-nitro-2-(3-phenylpropylamino)-benzoate; P_{dw}, diffusional water permeability; P_{urea}, urea permeabilities; rCLC-K1, specific chloride channel; RT-PCR, reverse transcription-polymerase chain reaction; TAL, thick ascending limb; tDL, thin descending limb; UT, urea transporter; V_D, diffusional voltage; VRC, vanadyl ribonucleoside complex; V_T, transepithelial voltage.

REFERENCES

1. Spitzer A, Schwartz G: The kidney during development, in *Handbook of Physiology: Renal Physiology* (vol 1), edited by Windhager E, New York, Oxford University Press, 1992, pp 475–544
2. Edwards BR, Mendel DB, LaRochelle FT Jr, *et al*: Postnatal development of urinary concentrating ability in rats: changes in renal anatomy and neurohypophysial hormones, in *The Kidney During Development: Morphology and Function*, edited by Spitzer A, New York, Masson, 1981, pp 233–240
3. Hamburger O: Uber dir Entwicklung der Saugetierniere. *Arch Anat Physiol* (Suppl)14:15–51, 1890
4. Kim J, Lee GS, Tisher CC, Madsen KM: Role of apoptosis in development of the ascending thin limb of the loop of Henle in rat kidney. *Am J Physiol* 271:F831–F845, 1996
5. Kondo Y, Abe K, Igarashi Y, *et al*: Direct evidence for the absence of active Na^+ reabsorption in hamster ascending thin limb of Henle's loop. *J Clin Invest* 91:5–11, 1993
6. Takahashi N, Kondo Y, Fujiwara I, *et al*: Characterization of Na^+ transport across the cell membranes of the ascending thin limb of Henle's loop. *Kidney Int* 47:789–794, 1995
7. Uchida S, Sasaki S, Nitta K, *et al*: Localization and functional characterization of rat kidney-specific chloride channel, ClC-K1. *J Clin Invest* 95:104–113, 1995
8. Matsumura Y, Uchida S, Kondo Y, *et al*: Overt nephrogenic diabetes insipidus in mice lacking the CLC-K1 chloride channel. *Nat Genet* 21:95–98, 1999
9. Vehaskari VM, Hempe JM, Manning J, *et al*: Developmental regulation of ENaC subunit mRNA levels in rat kidney. *Am J Physiol* 274:C1661–C1666, 1998
10. Yamamoto T, Sasaki S, Fushimi K, *et al*: Expression of AQP family in rat kidneys during development and maturation. *Am J Physiol* 272:F198–F204, 1997
11. Moriyama T, Murphy HR, Martin BM, Garcia-Perez A: Detection of specific mRNAs in single nephron segments by use of the polymerase chain reaction. *Am J Physiol* 258:F1470–F1474, 1990
12. Ma T, Frigeri A, Skach W, Verkman AS: Cloning of a novel rat kidney cDNA homologous to CHIP28 and WCH-CD water channels. *Biochem Biophys Res Commun* 197:654–659, 1993
13. Uchida S, Sasaki S, Furukawa T, *et al*: Molecular cloning of a chloride channel that is regulated by dehydration and expressed predominantly in kidney medulla. *J Biol Chem* 268:3821–3824, 1993
14. Gamba G, Miyanoshita A, Lombardi M, *et al*: Molecular cloning, primary structure, and characterization of two members of the mammalian electroneutral sodium-(potassium)-chloride cotransporter family expressed in kidney. *J Biol Chem* 269:17713–17722, 1994
15. Fushimi K, Uchida S, Hara Y, *et al*: Cloning and expression of apical membrane water channel of rat kidney collecting tubule. *Nature* 361:549–552, 1993
16. Shayakul C, Steel A, Hediger MA: Molecular cloning and characterization of the vasopressin-regulated urea transporter of rat kidney collecting ducts. *J Clin Invest* 98:2580–2587, 1996
17. Raff T, van der Giet M, Endemann D, *et al*: Design and testing of beta-actin primers for RT-PCR that do not co- amplify processed pseudogenes. *Biotechniques* 23:456–460, 1997
18. Burg M, Grantham J, Abramow M, Orloff J: Preparation and study of fragments of single rabbit nephrons. *Am J Physiol* 210:1293–1298, 1966
19. Kondo Y, Fromter E: Axial heterogeneity of sodium-bicarbonate cotransport in proximal straight tubule of rabbit kidney. *Pflügers Arch* 410:481–486, 1987
20. Kondo Y, Kudo K, Igarashi Y, *et al*: Functions of ascending thin limb of Henle's loop with special emphasis on mechanism of NaCl transport. *Tohoku J Exp Med* 166:75–84, 1992
21. Isozaki T, Yoshitomi K, Imai M: Effects of Cl^- transport inhibitors on Cl^- permeability across hamster ascending thin limb. *Am J Physiol* 257:F92–F98, 1989
22. Wangemann P, Wittner M, Di Stefano A, *et al*: Cl(−)-channel blockers in the thick ascending limb of the loop of Henle. Structure activity relationship. *Pflügers Arch* 407(Suppl):S128–S141, 1986
23. Haas M, Forbush B III: The Na-K-Cl cotransporters. *J Bioenerg Biomembr* 30:161–172, 1998
24. Farman N: Na,K-pump expression and distribution in the nephron. *Miner Electrolyte Metab* 22:272–278, 1996
25. Imai M, Taniguchi J, Yoshitomi K: Osmotic work across inner medullary collecting duct accomplished by difference in reflection coefficients for urea and NaCl. *Pflügers Arch* 412:557–567, 1988
26. Bondy C, Chin E, Smith BL, *et al*: Developmental gene expression and tissue distribution of the CHIP28 water-channel protein. *Proc Natl Acad Sci USA* 90:4500–4504, 1993
27. Karakashian A, Timmer RT, Klein JD, *et al*: Cloning and characterization of two new isoforms of the rat kidney urea transporter: UT-A3 and UT-A4. *J Am Soc Nephrol* 10:230–237, 1999
28. Carroll RL: *Patterns and Processes of Vertebrate Evolution*. Cambridge, Cambridge University Press, 1999
29. Hedges SB: Molecular evidence for the origin of birds. *Proc Natl Acad Sci USA* 91:2621–2624, 1994
30. Hedges SB, Poling LL: A molecular phylogeny of reptiles. *Science* 283:998–1001, 1999
31. Nigam SK, Aperia AC, Brenner BM: I Elements of normal renal structure and function 2 Development and Maturation of the Kidney, in *Brenner & Rector's The Kidney* (5th ed, vol I), edited by Brenner BM, Boston, Saunders, Harvard University, 1996, pp 72–98
32. Tisher CC, Madsen KM: I Elements of normal renal structure and function 1 Anatomy of the Kidney, in *Brenner & Rector's The Kidney* (5th ed, vol I), edited by Brenner BM, Boston, Saunders, Harvard University, 1996, pp 3–71
33. Morild I, Bohle A, Christensen JA: Structure of the avian kidney. *Anat Rec* 212:33–40, 1985
34. Nishimura H, Imai M, Ogawa M: Diluting segment in avian kidney. I. Characterization of transepithelial voltages. *Am J Physiol* 250:R333–R340, 1986

35. Miwa T, Nishimura H: Diluting segment in avian kidney. II. Water and chloride transport. *Am J Physiol* 250:R341–R347, 1986
36. Nishimura H, Koseki C, Imai M, Braun EJ: Sodium chloride and water transport in the thin descending limb of Henle of the quail. *Am J Physiol* 257:F994–F1002, 1989
37. Nishimura H, Koseki C, Patel TB: Water transport in collecting ducts of Japanese quail. *Am J Physiol* 271:R1535–R1543, 1996
38. Stanton BA: Characterization of apical and basolateral membrane conductances of rat inner medullary collecting duct. *Am J Physiol* 256:F862–F868, 1989
39. Imai M, Yoshitomi K: Electrophysiological study of inner medullary collecting duct of hamsters. *Pflügers Arch* 416:180–188, 1990
40. Nishimura H: Countercurrent urine concentration in birds, in *New Insight in Vertebrate Kidney Function*, edited by Brown JA, Balment RJ, Rankin JC, Cambridge, Cambridge University Press, 1993, pp 189–212